

TABLE OF CONTENTS

	Page
ACKNOWLEDGMENTS	iii
ABSTRACT (ENGLISH)	v
ABSTRACT (THAI)	vii
LIST OF TABLES	xiv
LIST OF ILLUSTRATIONS	xvi
ABBREVIATIONS AND SYMBOLS	xxvi
CHAPTER 1 INTRODUCTION	1
1.1 Thesis rationale	1
1.2 Purpose of the research	3
1.3 Organization of the thesis	4
CHAPTER 2 LITERATURE REVIEWS	6
2.1 Ferroelectrics crystal structure and ferroelectricity	6
2.1.1 Normal ferroelectrics	10
2.1.2 Relaxor ferroelectrics	12
2.2 Perovskite materials	17
2.2.1 Lead zirconate titanate ($\text{Pb}(\text{Zr},\text{Ti})\text{O}_3$ or PZT)	22
2.2.2 Modification by doping	25
2.2.3 Modification PZT by relaxor ferroelectric	36
2.2.4 Lead zinc niobate ($\text{Pb}(\text{Zn}_{1/3}\text{Nb}_{2/3})\text{O}_3$ or PZN)	38

	Page
2.3 Figures of merit in piezoelectrics	42
2.4 Drive/Control techniques	44
CHAPTER 3 EXPERIMENTAL PROCEDURES	46
3.1 Sample preparation	46
3.1.1 Powder preparation	46
3.1.2 Ceramic preparation	48
3.2 Sample characterization	49
3.2.1 Physical properties	49
3.2.2 Electrical properties	54
CHAPTER 4 PHYSICAL AND ELECTRICAL PROPERTIES OF PZN-PZT BASED COMPOSITION	58
4.1 Synthesis, formation and characterization of PZN-PZT powders	58
4.1.1 Experimental procedure	59
4.1.2 Results and discussion	61
4.1.2.1 Thermogravimetric and Differential Thermal Analysis (TG/DTA)	62
4.1.2.2 X-Ray Diffraction Analysis (XRD)	63
4.1.2.3 SEM and EDX Analysis	66
4.1.3 Summary	67

	Page
4.2 Effect of PZN content on properties of PZN-PZT based ceramics	68
4.2.1 Experimental procedure	69
4.2.2 Results and discussion	70
4.2.2.1 Crystal structure, phase formations and microstructure	70
4.2.2.2 Dielectric properties	74
4.2.2.3 Piezoelectric properties	80
4.2.2.4 Ferroelectric properties	82
4.2.3 Summary	85
4.3 Effect of Zr/Ti ratio content on properties of PZN-PZT based ceramics	85
4.3.1 Experimental procedure	86
4.3.2 Results and discussion	87
4.3.2.1 Crystal structure, phase formations and microstructure	87
4.3.2.2 Dielectric properties	90
4.3.2.3 Piezoelectric properties	96
4.3.2.4 Ferroelectric properties	97
4.3.3 Summary	100

	Page
CHAPTER 5 PHYSICAL AND ELECTRICAL PROPERTIES OF MODIFIED PZN-PZT BASED COMPOSITION	101
5.1 Effect of MnO₂ addition on properties of PZN-PZT ceramics	101
5.1.1 Experimental procedure	102
5.1.2 Results and discussion	103
5.1.2.1 Crystal structure, phase formations and microstructure	103
5.1.2.2 Dielectric properties	107
5.1.2.3 Piezoelectric properties	109
5.1.2.4 Ferroelectric properties	111
5.1.3 Summary	114
5.2 Effect of Fe₂O₃ addition on properties of PZN-PZT ceramics	114
5.2.1 Experimental procedure	115
5.2.2 Results and discussion	116
5.2.2.1 Crystal structure, phase formations and microstructure	116
5.2.2.2 Dielectric properties	119
5.2.2.3 Piezoelectric properties	122

	Page
5.2.2.4 Ferroelectric properties	123
5.2.3 Summary	126
5.3 Comparison between Fe₂O₃ and MnO₂ addition on properties of PZN-PZT ceramics	126
5.3.1 Experimental procedure	127
5.3.2 Results and discussion	128
5.3.2.1 Crystal structure, phase formations and microstructure	128
5.3.2.2 Dielectric properties	130
5.3.2.3 Piezoelectric properties	133
5.3.2.4 Ferroelectric properties	134
5.3.3 Summary	135
CHAPTER 6 CONCLUSIONS AND FUTURE WORK	136
6.1 Conclusions	136
6.1.1 PZN-PZT based compositions	136
6.1.2 Modified PZN-PZT compositions	137
6.2 Future work	139
REFERENCES	141
APPENDIX	148
VITA	150

LIST OF TABLES

Table		Page
2.1	Crystallographic classification scheme based on polarity and the presence of a center of symmetry.	9
2.2	Property differences between relaxor and normal perovskite ferroelectrics.	14
2.3	Common doping effect for PZT ceramics relative to undoped PZT ceramic.	26
2.4	Radii of soft dopant ions.	29
2.5	Radii of hard dopant ions.	31
2.6	Advantages (+) and disadvantages (–) of soft and hard piezoelectrics, compared with the features of a leading electrostrictive material.	36
2.7	Ternary piezoelectric ceramics compositions.	37
3.1	Specifications of the component oxide powders used in this study.	47
4.1	Percentage of perovskite phase of $x\text{PZN}-(1-x)\text{PZT}$; $x = 0.1-0.5$.	65
4.2	Physical properties of $x\text{PZN}-(1-x)\text{PZT}$ ceramics.	73
4.3	Dielectric properties of $x\text{PZN}-(1-x)\text{PZT}$ ceramics.	80
4.4	Piezoelectric, ferroelectric and strain properties of $x\text{PZN}-(1-x)\text{PZT}$ ceramics.	81
4.5	Physical properties of $0.2\text{Pb}(\text{Zn}_{1/3}\text{Nb}_{2/3})\text{O}_3-0.8\text{Pb}(\text{Zr}_x\text{Ti}_{1-x})\text{O}_3$ ceramics.	90

Table	Page
4.6 Dielectric properties of $0.2\text{Pb}(\text{Zn}_{1/3}\text{Nb}_{2/3})\text{O}_3\text{-}0.8\text{Pb}(\text{Zr}_x\text{Ti}_{1-x})\text{O}_3$ ceramics.	94
4.7 Piezoelectric properties of $0.2\text{Pb}(\text{Zn}_{1/3}\text{Nb}_{2/3})\text{O}_3\text{-}0.8\text{Pb}(\text{Zr}_x\text{Ti}_{1-x})\text{O}_3$ ceramics.	96
5.1 Physical Properties of $0.2\text{PZN}\text{-}0.8\text{PZT} + x \text{ wt}\% \text{ MnO}_2$ ceramics.	105
5.2 Dielectric and piezoelectric properties of $0.2\text{PZN}\text{-}0.8\text{PZT} + x \text{ wt}\% \text{ MnO}_2$ ceramics.	111
5.3 Ferroelectric and strain properties of $0.2\text{PZN}\text{-}0.8\text{PZT} + x \text{ wt}\% \text{ MnO}_2$ ceramics.	113
5.4 Physical properties of $0.2\text{PZN}\text{-}0.8\text{PZT} + x \text{ wt}\% \text{ Fe}_2\text{O}_3$ ceramics.	119
5.5 Dielectric and piezoelectric properties of $0.2\text{PZN}\text{-}0.8\text{PZT} + x \text{ wt}\% \text{ Fe}_2\text{O}_3$ ceramics.	121
5.6 Ferroelectric and strain properties of $0.2\text{PZN}\text{-}0.8\text{PZT} + x \text{ wt}\% \text{ Fe}_2\text{O}_3$ ceramics.	124
5.7 Physical properties of $0.2\text{PZN}\text{-}0.8\text{PZT}$ ceramics.	130
5.8 Dielectric and Piezoelectric properties of $0.2\text{PZN}\text{-}0.8\text{PZT}$ ceramics.	132
5.9 Ferroelectric and strain properties of $0.2\text{PZN}\text{-}0.8\text{PZT}$ ceramics.	135

LIST OF ILLUSTRATIONS

Figure		Page
2.1	Microscopic origins of the electric polarization.	7
2.2	Polarization of the material depends on the frequency of the applied field.	7
2.3	Venn diagram of electroceramics properties.	9
2.4	A typical ferroelectric hysteresis loop.	10
2.5	A general depiction of the temperature dependences of the spontaneous polarization, the dielectric constant, and the inverse dielectric constant for a ferroelectric. (a) second-order phase transitions and (b) first-order phase transitions	11
2.6	Crystal structure models of the $A(B_{1/2}^I B_{1/2}^{II})O_3$ type perovskite: (a) the ordered structure with a small rattling space and (b) the disordered structure with a large rattling space [open circle = B^I (lower valence cation) and solid circle = B^{II} (higher valence cation)].	16
2.7	The temperature dependence of the permittivity and $\tan \delta$ in $Pb(Mg_{1/3}Nb_{2/3})O_3$ for the various measuring frequencies from 0.1kHz -1MHz	17
2.8	The perovskite crystal structure.	18
2.9	Classification of the perovskite $A^{2+}B^{4+}O^{2-}_3$ - type compounds according to the constituent ionic radii.	19

Figure	Page
2.10 Order arrangement of B-site ions in complex perovskites: (a) simple type, (b) 1:1 order type, (c) 1:2 order type.	20
2.11 Electronegativity difference versus tolerance factor for ABO_3 perovskite compounds.	21
2.12 $PbTiO_3$ - $PbZrO_3$ sun-solidus phase diagram.	22
2.13 Lattice parameters at room temperature for the $PbZrO_3$ - $PbTiO_3$ system.	23
2.14 Possible orientation state in perovskites.	24
2.15 Composition dependence of dielectric constant and electromechanical coupling factor in PZT system.	24
2.16 (a) Variation of piezoelectric coefficient d_{ij} and (b) remanent polarization P_r with composition of PZT near the morphotropic phase boundary.	25
2.17 Crystal deficiencies in PZT for acceptor (a) and donor (b) dopants.	26
2.18 Variation of the coupling factor k_p in $Pb(Zr_{0.52}Ti_{0.48})O_3$ piezoelectric ceramics with various doping amounts of Nb_2O_5	27
2.19 Variation of the piezoelectric properties in the $0.05Pb(Sc_{1/2}Ta_{1/2})O_3$ - $0.455PbTiO_3$ - $0.495PbZrO_3$ ceramics with various doping amounts of MnO_2 .	30

Figure	Page
2.20 Variation of the dielectric loss in a PZT piezoelectric ceramics with difference doping amounts of Fe_2O_3 .	31
2.21 Effect of poling temperature on the coupling factor k_p in the $\text{Pb}(\text{Zr}_{0.52}\text{Ti}_{0.48})\text{O}_3$ piezoelectric ceramics with various doping amounts of Cr_2O_3 .	33
2.22 Effect of complex doping of both NiO and MnO_2 on the piezoelectric properties of the $\text{Pb}(\text{Zn}_{1/3}\text{Nb}_{2/3})_{0.2}\text{Ti}_{0.36}\text{Zr}_{0.44}\text{O}_3$ ceramics.	34
2.23 Ternary diagram depicting MPBs in $\text{Pb}(\text{Zr,Ti})\text{O}_3$ and relaxor ferroelectric systems for piezoelectric ceramics.	37
2.24 Possible range of planar coupling k_p and mechanical quality factor Q_m for modified PZT and ternary composition.	38
2.25 Classification of piezoelectric/electrostrictive actuators.	45
3.1 Diagram of experimental procedure on powder preparation.	48
3.2 Diagram of experimental procedure on ceramic preparation.	49
3.3 Diagram of experimental procedure on sample characterization.	49
3.4 Differential thermal analysis (Perkin Elmer DTA7)	50
3.5 Thermogravimetric analysis (Perkin Elmer TGA7)	50
3.6 X-ray diffractometer	51
3.7 Scanning electron microscope.	52
3.8 Dielectric Measurements system.	54

Figure	Page
3.9 Poling system.	54
3.10 Quasi-static piezoelectric d_{33} meter.	55
3.11 Impedance analyzer HP4294A.	55
3.12 Ferroelectric and strain measurements.	57
3.13 Conceptual block diagram	57
4.1 Diagram of experimental procedure.	61
4.2 TG-DTA curves for the mixture of PbO-ZnO-Nb ₂ O ₅ -ZrTiO ₂ -TiO ₂ powder.	62
4.3 XRD patterns of 0.5PZN–0.5PZT powder calcined at various temperatures for 2 h. with heating/cooling rates of 20°C/min.	63
4.4 XRD patterns of the x PZN -(1- x)PZT powders (when $x = 0.1, 0.2, 0.3, 0.4,$ and 0.5) calcined at 900°C with heating/cooling rates of 20°C/min and soaking time of 2 h.	64
4.5 SEM micrographs of the x PZN-(1- x)PZT powders calcined at 900°C with heating/cooling rates of 20°C/min and soaking time of 2 h for (a) $x=0.1$, (b) $x=0.2$, (c) $x=0.3$, (d) $x=0.4$ and (e) $x=0.5$.	66
4.6 EDX analysis of the 0.2PZN-0.8PZT powders calcined at 900°C with heating/cooling rates of 20°C/min and soaking time of 2 h	67
4.7 (a) XRD diffraction patterns of sintered x PZN-(1 - x)PZT ceramics. (b) selected region of the diffraction patterns.	72

Figure	Page
4.8 SEM micrographs of x PZN-(1- x)PZT ceramics with various compositions: (a) $x = 0.1$, (b) $x = 0.2$, (c) $x = 0.3$, (d) $x = 0.4$, and (e) $x = 0.5$.	74
4.9 Temperature and frequency dependence of dielectric properties of x PZN-(1- x)PZT ceramics ;(a) $x = 0.1$, (b) $x = 0.2$, (c) $x = 0.3$, (d) $x = 0.4$, and (e) $x = 0.5$.	75
4.10 Temperature dependence of dielectric properties of x PZN-(1- x)PZT ceramics at 1kHz.	76
4.11 T_m calculated and T_m from maximum ϵ_r as a function of composition x at 1 kHz.	77
4.12 Dependence of $\log [(\epsilon_m/\epsilon_r)-1]$ with $\log(T-T_m)$ for x PZN-(1- x)PZT ceramics.	79
4.13 Dependence of diffusivity (γ) and diffuseness parameter (δ) for x PZN-(1- x)PZT ceramics.	79
4.14 Density, dielectric constant (ϵ_r), piezoelectric constant (d_{33}), electromechanical coupling factor (k_p), and mechanical quality factor (Q_m) of x PZN-(1- x)PZT ceramics.	81
4.15 Polarization and electric field of x PZN-(1- x)PZT ceramics with $x = 0.1-0.5$.	83

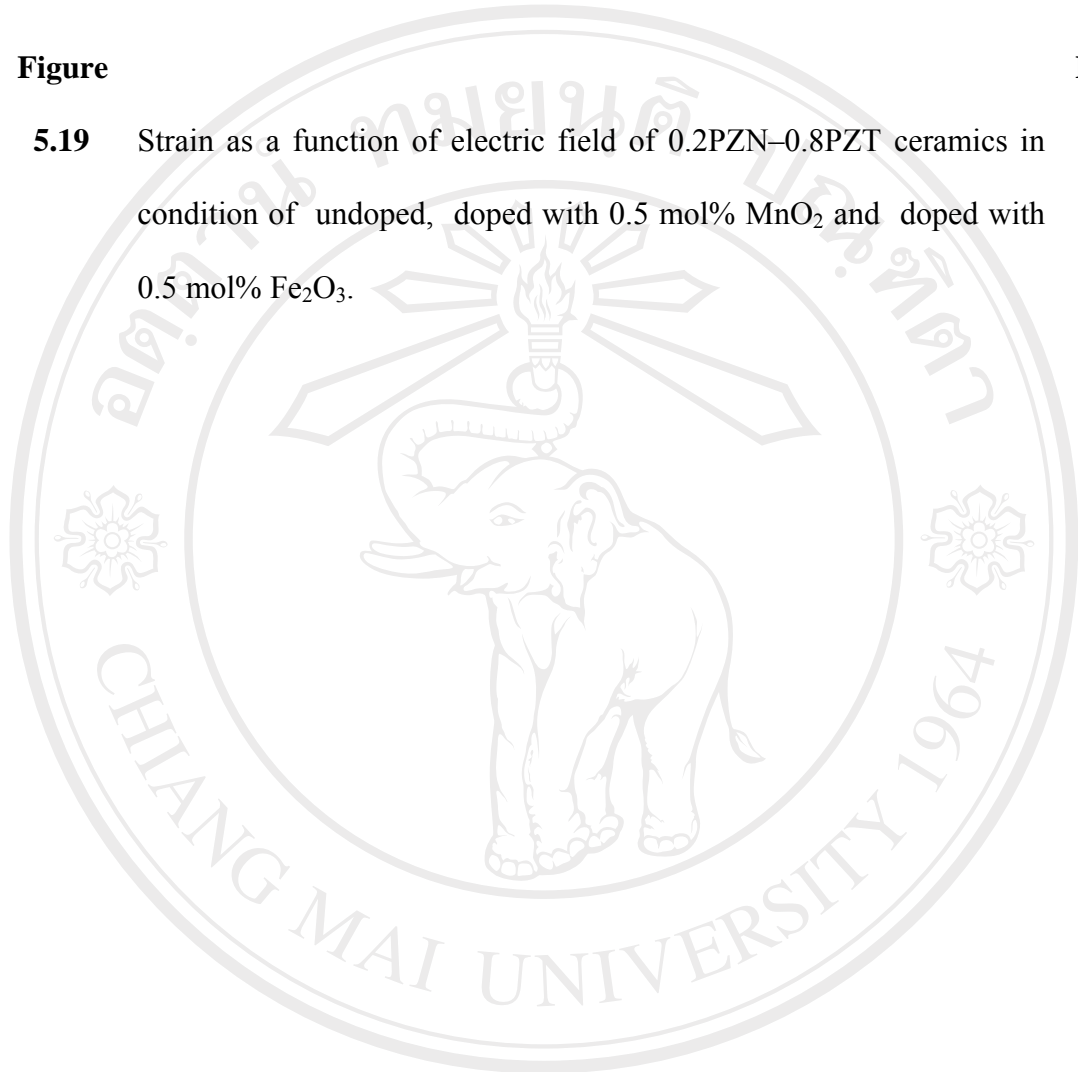
Figure	Page
4.16 Strain and electric field of x PZN-(1- x)PZT ceramics with $x = 0.1-0.5$.	84
4.17 (a) XRD diffraction patterns of sintered $0.2\text{Pb}(\text{Zn}_{1/3}\text{Nb}_{2/3})\text{O}_3$ - $0.8\text{Pb}(\text{Zr}_x\text{Ti}_{1-x})\text{O}_3$ ceramics. (b) selected region of the diffraction patterns.	88
4.18 SEM micrographs $0.2\text{Pb}(\text{Zn}_{1/3}\text{Nb}_{2/3})\text{O}_3$ - $0.8\text{Pb}(\text{Zr}_x\text{Ti}_{1-x})\text{O}_3$ ceramics with various compositions: (a) $x = 0.40$, (b) $x = 0.45$, (c) $x = 0.50$, (d) $x = 0.52$, (e) $x = 0.55$, and (f) $x = 0.60$.	89
4.19 Temperature and frequency dependence of dielectric properties of $0.2\text{Pb}(\text{Zn}_{1/3}\text{Nb}_{2/3})\text{O}_3$ - $0.8\text{Pb}(\text{Zr}_x\text{Ti}_{1-x})\text{O}_3$ ceramics; (a) $x = 0.40$, (b) $x = 0.45$, (c) $x = 0.50$, (d) $x = 0.52$, (e) $x = 0.55$, and (f) $x = 0.60$.	91
4.20 Temperature dependence of dielectric properties of $0.2\text{Pb}(\text{Zn}_{1/3}\text{Nb}_{2/3})\text{O}_3$ - $0.8\text{Pb}(\text{Zr}_x\text{Ti}_{1-x})\text{O}_3$ ceramics at 1kHz.	92
4.21 T_m calculated and T_m from maximum ϵ_r as a function of composition x at 1 kHz.	93
4.22 Dependence of $\log [(\epsilon_m/\epsilon)-1]$ with $\log(T-T_m)$ for $0.2\text{Pb}(\text{Zn}_{1/3}\text{Nb}_{2/3})\text{O}_3$ - $0.8\text{Pb}(\text{Zr}_x\text{Ti}_{1-x})\text{O}_3$ ceramics.	95
4.23 Dependence of diffusivity (γ) and diffuseness parameter (δ) for $0.2\text{Pb}(\text{Zn}_{1/3}\text{Nb}_{2/3})\text{O}_3$ - $0.8\text{Pb}(\text{Zr}_x\text{Ti}_{1-x})\text{O}_3$ ceramics	95

Figure	Page
4.24 Density, dielectric constant (ϵ_r), piezoelectric constant (d_{33}), electromechanical coupling factor (k_p), and mechanical quality factor (Q_m) of $0.2\text{Pb}(\text{Zn}_{1/3}\text{Nb}_{2/3})\text{O}_3$ - $0.8\text{Pb}(\text{Zr}_x\text{Ti}_{1-x})\text{O}_3$ ceramics.	97
4.25 Polarization and electric field of $0.2\text{Pb}(\text{Zn}_{1/3}\text{Nb}_{2/3})\text{O}_3$ - $0.8\text{Pb}(\text{Zr}_x\text{Ti}_{1-x})\text{O}_3$ ceramics	98
4.26 Strain and electric field of $0.2\text{Pb}(\text{Zn}_{1/3}\text{Nb}_{2/3})\text{O}_3$ - $0.8\text{Pb}(\text{Zr}_x\text{Ti}_{1-x})\text{O}_3$ ceramics	99
5.1 XRD patterns of the samples sintered at 1200°C for 2h in of 0.2PZN - $0.8\text{PZT} + x \text{ wt}\% \text{MnO}_2$ ceramics: (a) $x = 0$, (b) $x = 0.1$, (c) $x = 0.3$, (d) $x = 0.5$, (e) $x = 0.7$ and (f) $x = 0.9$.	104
5.2 SEM images of the specimens sintered surface of 0.2PZN - $0.8\text{PZT} + x \text{ wt}\% \text{MnO}_2$ ceramics at 1200°C for 2h;(a) $x = 0$, (b) $x = 0.1$, (c) $x = 0.3$, (d) $x = 0.5$, (e) $x = 0.7$ and (f) $x = 0.9$.	106
5.3 Temperature and frequency dependence of dielectric properties of 0.2PZN - $0.8\text{PZT} + x \text{ wt}\% \text{MnO}_2$ ceramics at 1200°C for 2h; (a) $x = 0$, (b) $x = 0.1$, (c) $x = 0.3$, (d) $x = 0.5$, (e) $x = 0.7$ and (f) $x = 0.9$.	108
5.4 Curie temperature of the specimens sintered at 1200°C for 2h of 0.2PZN - $0.8\text{PZT} + x \text{ wt}\% \text{MnO}_2$ ceramics when $x = 0$, 0.1 , 0.3 , 0.5 , 0.7 and 0.9 .	109

Figure	Page
5.5 Density, dielectric constant (ϵ_r), piezoelectric constant (d_{33}), electromechanical coupling factor (k_p), and mechanical quality factor (Q_m) of the specimens sintered at 1200°C for 2h of 0.2PZN–0.8PZT + x wt% MnO ₂ ceramics when $x = 0, 0.1, 0.3, 0.5, 0.7$ and 0.9 .	110
5.6 Polarization and electric field of 0.2PZN–0.8PZT + x wt% MnO ₂ ceramics.	112
5.7 Strain and electric field of 0.2PZN–0.8PZT + x wt% MnO ₂ ceramics.	113
5.8 XRD patterns of the samples sintered at 1200°C for 2h in 0.2PZN–0.8PZT + x wt% Fe ₂ O ₃ ceramics : (a) $x = 0$, (b) $x = 0.1$, (c) $x = 0.3$, (d) $x = 0.5$, (e) $x = 0.7$ and (f) $x = 0.9$.	117
5.9 SEM images of the specimens sintered surface of 0.2PZN–0.8PZT + x wt% Fe ₂ O ₃ ceramics at 1200°C for 2h;(a) $x = 0$, (b) $x = 0.1$, (c) $x = 0.3$, (d) $x = 0.5$, (e) $x = 0.7$ and (f) $x = 0.9$.	118
5.10 Temperature and frequency dependence of dielectric properties of 0.2PZN–0.8PZT + x wt% Fe ₂ O ₃ ceramics at 1200°C for 2h; (a) $x = 0$, (b) $x = 0.1$, (c) $x = 0.3$, (d) $x = 0.5$, (e) $x = 0.7$ and (d) $x = 0.9$.	120
5.11 Curie temperature of the specimens sintered at 1200°C for 2h of 0.2PZN–0.8PZT + x wt% Fe ₂ O ₃ ceramics when $x = 0, 0.1, 0.3, 0.5, 0.7$ and 0.9 .	121

Figure	Page
5.12 Density, dielectric constant (ϵ_r), piezoelectric constant (d_{33}), electromechanical coupling factor (k_p), and mechanical quality factor (Q_m) of the specimens sintered at 1200°C for 2h in 0.2PZN–0.8PZT + x wt% Fe ₂ O ₃ ceramics; when $x = 0, 0.1, 0.3, 0.5, 0.7$ and 0.9 .	123
5.13 Polarization and electric field 0.2PZN–0.8PZT + x wt% Fe ₂ O ₃ ceramics.	125
5.14 Strain and electric field of 0.2PZN–0.8PZT + x wt% Fe ₂ O ₃ ceramics.	125
5.15 XRD patterns of the samples sintered at 1200°C for 2h in 0.2PZN–0.8PZT ceramics: (a) undoped, (b) doped with 0.5mol% MnO ₂ and (c) doped with 0.5mol% Fe ₂ O ₃ .	128
5.16 SEM images of the specimens sintered surface of 0.2PZN–0.8PZT ceramics at 1200°C for 2h; (a) undoped, (b) doped with 0.5 mol% MnO ₂ and (c) doped with 0.5 mol% Fe ₂ O ₃	129
5.17 Temperature and frequency dependence of dielectric properties of 0.2PZN–0.8PZT ceramics at 1200°C for 2h : (a) undoped, (b) doped with 0.5 mol% MnO ₂ and (c) doped with 0.5 mol% Fe ₂ O ₃ .	131
5.18 Polarization as a function of electric field of 0.2PZN–0.8PZT ceramics in condition of undoped, doped with 0.5 mol% MnO ₂ and doped with 0.5 mol% Fe ₂ O ₃ .	134

Figure	Page
5.19 Strain as a function of electric field of 0.2PZN–0.8PZT ceramics in condition of undoped, doped with 0.5 mol% MnO ₂ and doped with 0.5 mol% Fe ₂ O ₃ .	134



ลิขสิทธิ์มหาวิทยาลัยเชียงใหม่
Copyright© by Chiang Mai University
All rights reserved

ABBREVIATIONS AND SYMBOLS

a	lattice parameter a
ac	alternating current
A	area
C	Curie-Weiss constant
c	capacitance
dc	direct current
d_{ij}	piezoelectric coefficients
E	electric field ($V\ m^{-1}$); strain
ΔEN	electronegativity
E_c	Coercive field
e	electron charge
f	frequency
f_a	anti-resonance frequency
f_r	resonance frequency
I_{perov}	maximum intensity of perovskite phase
I_{pyro}	maximum intensity of pyrochlore phase
K_α	radiation of K series
k_{ij}	electromechanical coupling
LCR	Inductance/Capacitance/Resistance
MPB	Morphotropic Phase Boundaries
$P-E$	Polarization versus electric field

P_s	spontaneous polarization
P_r	remanent polarization
SEM	scanning electron microscopy
s_{ij}	field-induced strain
T_0	Curie-Weiss temperature
T_m	temperature at maximum permittivity
T_c	Curie point
t	thickness; tolerance factor
$\tan \delta$	loss tangent
XRD	x-ray diffraction
X_{A-O}	electronegativity differences of cation A and oxygen
X_{B-O}	electronegativity differences of cation B and oxygen
δ	diffuseness parameter
ϵ_0	permittivity of free space
ϵ_r	relative permittivity
ϵ_{\max}	the permittivity at T_{\max}
γ	critical exponent or diffusivity
δ	diffuseness